

Study On Green Synthesis And Characterization Of Copper, Manganese Nanoparticles In *T.Populnea* For Biomedical Applications

Sara Palaparthi^{1*}, Prof. B.Sujatha²

^{1*}Lecturer in Botany, Government Degree College, Ramachandrapuram, 533250 Email:-sharagiridhar@gmail.com, 7386379223

²Professor in Botany, Andhra University, Visakhapatnam, 530003 Email:-prof.bsujatha@andhrauniversity.edu.in, 9440425270

ABSTRACT: -

Nanotechnology is a broad interdisciplinary field with many applications in science & technology. These Nanoparticles are 1-100nm in dimension. Locally available plant namely *Thespesia populnea* commonly called Portia tree leaves and figs were taken for nanoparticle isolation. The solvent most widely used are water, Copper sulphate & Manganese oxide mixture at P^H 5-7, temperature between 50-70⁰ C and Concentrations 1:2, 1:3 respectively. The mixtures after incubation centrifuged and the pellet was dried in oven at 70⁰C for 2hours and the formed copper and Manganese nanoparticles were isolated. Totally 32 samples of copper & Manganese nanoparticles with different parameters have been collected. 0.1g of each sample is taken and 1ml of DMSO (Dimethyl Sulfoxide) to each tube and mixed them thoroughly. Then 10 μ l of the prepared solution was added and the sample is subjected to UV-Visible spectrophotometer at 200nm, 220nm, 240nm, 250nm, 300nm, 350nm and 400nm, SEM at 500 – 94,300X, XRD at $2\theta = 10^0 - 90^0$ for characterization. Antibacterial and antifungal activity performed i.e sterilized and solidified nutrient agar and PDA loaded with 100 μ l of Gram positive bacteria, Gram negative bacteria, fungal organisms through disc diffusion method. Cu NP's acts against upon Gram positive Bacteria *Clostridium Perfringens*, Gram negative Bateria *Aeromonas hydrophila*, *Salmonella enterica* & Fungi like *Phytophthora infestans* and Mn NP's acts against upon Gram positive bacteria *Bacillus subtilis* , Gram negative bacteria *Salmonella enterica* & Fungi like *Candida albicans*

Keywords:- *Thespesia populnea*, Nanoparticles, Copper Sulphate, Manganese oxide, DMSO, UV-Visible spectrophotometer, SEM, XRD, PDA

1. INTRODUCTION: -

Nanotechnology is the multidisciplinary science in which the particles size ranges from 1- 100nm. These particles show peculiar properties rather than macro particles (L. K. Hakim et.al., 2021). The documented uses of such nanoparticles have expanded across various scientific domains including food science, pharmaceuticals, healthcare, engineering, and notably agriculture, primarily driven by advancements in chemical synthesis methods, which, when combined with alternative synthesis approaches, could streamline and expedite nanoparticle production (J. A. Gerbec et.al., 2005). Due to their elevated surface energy, nanoparticles exhibit considerable reactivity and thermodynamic instability (J.-P. Jolivet et.al., 2004). Hence, there exist multiple incentives for synthesizing, advancing, and bringing nanoparticles to market (A. K. Gupta et.al., 2005). While NP offer advantageous effects (G. Oberdörster et.al., 2005, A. Nel et.al., 2006), there is also apprehension regarding their potential toxicity to both humans, and plants (D. Lin et.al., 2008). Nanoparticles typically showcase distinct physiochemical characteristics, such as optical, thermal, and electrical properties, which vary from those of bulk particles (A. Rastogi et.al., 2017). In general, the construction of nanoparticles involves the incorporation of reducing or precipitating agents throughout their synthesis (M. Sanchez-Dominguez et.al., 2009). The emergence of green synthesis techniques for nanomaterials, devoid of harmful chemicals, has emerged as a prominent focus within nanoscience research, fostering the advancement of eco-friendly methodologies (M. P´erez-Alvarez et.al., 2021). (H. Kumar et.al., 2022) Green synthesis, specifically plant-mediated nanoparticle synthesis, has emerged as a feasible substitute for physical and chemical approaches. In contrast to conventional methods, it offers a straightforward, expeditious process employing less hazardous and environmentally friendly substances. Moreover, beyond alleviating environmental issues like solar interaction, catalysis, and agricultural output, green synthesis enhances the generation of renewable energy. Different plants, such as *Aloevera*, *Punica granatum*, and *Allium sativum*, have been employed in the synthesis of Cu nanoparticles. (Velázquez-Salazar et.al., 2017) As previously mentioned, while numerous techniques exist for environmentally friendly nanoparticle synthesis, only a limited number have been employed for manganese synthesis. Given the range of manganese oxide structures and the diverse organisms utilized for green synthesis, further investigation into the green synthesis of manganese nanoparticles holds potential interest. (Sharma et.al., 2019) Considering environmental factors, the utilization of green methods for synthesizing manganese nanoparticles is favored, as they obviate the need for specific chemical stabilizers and reducers, while enabling preparation under mild ambient temperature

and pressure conditions. (Iravani, S et.al., 2014) In biological synthesis of Mn NPs, raw materials such as vegetables, fruits, plant extracts, microbes, and fungi are employed to fabricate Mn and Mn-oxide nanoparticles, allowing for control over their shape and size. (Saranyaadevi et al., 2014) conducted a comprehensive study on the synthesis and characterization of copper nanoparticles utilizing *Capparis zeylanica* leaf extract. The characterization of the nanoparticles included various analyses such as UV-Vis spectroscopy, which confirmed the formation of nanoparticles through the observation of characteristic absorption peaks. Additionally, techniques such as X-ray diffraction (XRD) were employed to determine the crystalline structure of the nanoparticles. Further characterization through Scanning Electron Microscopy (SEM) allowed for the determination of particle size, shape, and distribution, elucidating the efficacy of the green synthesis approach employed. (Zhang et.al., 2019) Thus shape, crystallinity and structure of the amorphous and crystalline MnOx nanostructures were characterized in detail by X-ray diffraction (XRD), scanning electron microscopy (SEM). (S. Jin et.al., 2018, L. Ren et.al., 2015, Y. Zhuang et.al., 2020). In light of copper's essential role in the body, researchers have increasingly sought to leverage its beneficial effects in developing novel biomedical materials aimed at enhancing human health. Numerous investigations have demonstrated the outstanding properties of copper-containing metallic biomaterials in safeguarding the cardiovascular system, exhibiting antibacterial properties, and facilitating the healing of bone fractures. (Y. Chen et.al., 2020) Due to their physical and chemical properties, biocompatibility, and adjustable structure and morphologies, manganese oxides have garnered attention in various applications such as biosensing, bioimaging, drug delivery, and tumor therapy.

2. Materials&Methods:

2.1 Materials: -

Leaves and figs of the *Thespesia populnea* tree

0.2M CuSO₄.5H₂O, DMSO (Dimethyl Sulfoxide), MnO₂, Nutrient agar media, Ethanol, Potato Dextrose agar, Double distilled water, PH Meter

2.2 Synthesis of Cu Nanoparticles: -

0.2M CuSO₄.5H₂O solution was prepared by dissolving the 12.5g of CuSO₄.5H₂O in 250ml of distilled water in a beaker. The plant extracts of leaves and figs and 0.2M CuSO₄.5H₂O solution were mixed in 1:2 and 1:3 ratios in conical flasks separately and maintained the solution pH at 5-5.5 and covered them with aluminum foil and kept them in water bath for 30 minutes at temperature 50⁰C – 70⁰C. Then the mixtures were taken out from water bath and incubated the mixtures at room temperature for 24 hours. Copper nanoparticles were purified using centrifugation at 4000 rpm for 40 minutes and supernatant was discarded and pellet was dried in hot air oven at 70⁰C for 2hrs. (Sathish kumar et.,al 2010)

2.3 Synthesis of Mn Nanoparticles:

The plant extracts of leaves and figs were mixed with MnO₂ by taking 25ml of plant leaves and figs extracts into the conical flasks separately and 0.1gms of MnO₂ was added into each flasks separately and 0.1 gm of MnO₂ was added into each flask and the PH was maintained at 7.1-7.6 and covered them with the aluminum foil and kept them in water bath for 70 minutes at 40⁰C - 60⁰C. Then the mixtures were taken out from the water bath and observed the change of solution color that indicates the formation of nanoparticles. (Narayanan et.,al 2010). MnNPs were purified using centrifugation at 3000rpm for 30mts, supernatant was discarded and pellet was dried in Hot air Oven at 70⁰C for 2hrs.

3. Characterization of Cu, Mn NPs

3.1 UV-Visible Spectroscopy:-

16 Eppendorf tubes are taken and labelled with different parameters for each Nanoparticle. 0.1gm of both Cu Mn NPs are mixed with DMSO to each tube and 10 μ l of sample is taken into quartz cuvet and 1ml of distilled water is added and mixed thoroughly. Readings are taken through UV-Visible spectrophotometer at 200-400nm. UV-Vis spectroscopy is an excellent tool for identifying them is unique peak appears at a specific wavelength of light due to SRP electrons present on NP surfaces. (S. Brunauer et.,al 1938). Optical properties of Mn NPs and concentration is estimated by using UV-Vis spectroscopy. (Al-Douri et.,al 2018)

3.2. XRD Analysis of Cu, Mn NPs :-

As a radiation source, Cu K α (λ =1.540 $^{\circ}$ A) served as a crystallographic analyzer for the Cu NPs with a scan speed of 0.4 $^{\circ}$ /min and a 2 θ =10–700 radiation source. By identifying the compound's crystal structure and chemical composition using XRD analysis, the compound was identified. X-ray energy-dispersive spectroscopy was also used to assess the chemistry of nanoparticles. (D. B. Williams et., al 2009).

3.3. SEM Analysis of Cu, Mn NPs :-

Scanning electron microscopes (SEM) was used to obtain the morphological images of a wide variety of samples. This method allows sample images to be collected in the magnification range of 10 X to 250,000 X. Microphotographs of nanocomposites were appeared due to beam of high energy electron. Interaction of electrons with the atoms of the sample produce signals which shows the composition and surface morphology of the synthesized nanocomposites. SEM can achieve resolution better than nanometer. Specimen can be observed in a wet condition. The scattered electrons provide a lot of information about surface morphology of the sample and some are detected by detector. (M. Kuno et., al)

3.4 Anti-bacterial activity of Cu, Mn nanoparticles:

The Nutrient agar media was prepared by taking 100ml of distilled water into the conical flask and 1.3gms of nutrients were added to the distilled water in the conical flask mixed properly and 2gms of agar was added to the mixture. Then a cotton plug was made at the mouth of the conical flask was covered with it. Then the petri dishes were cleaned neatly by using ethanol and they were packed in a cover properly. Then the prepared media and plates were kept in autoclave and they were sterilized at 121°C temperature and 15lbs pressure for 15minutes. Media was poured into petri plates and left for 10-15mts for solidification. 100µl of microorganisms were taken and spread in plates with L-shaped rod, wells were made in plates with cork borer. 10µl of the respective Cu and Mn nanoparticles solutions were loaded to the respective wells and the plates were kept in incubator at 37°C for the growth of the microorganism and the anti-bacterial activity in the plates was observed with the zone of inhibition and was measured around each well and noted down. The anti-bacterial activity was done with 5 gram-negative bacteria named *Bacillus subtilis*, *Bacillus licheniformis*, *Clostridium perfringens*, *Staphylococcus epidermidis*, *Staphylococcus aureus* and 5 gram-positive bacteria named *Aeromonas hydrophila*, *vibrio cholera*, *Escherichia coli*, *pseudomonas aeruginosa*, *Salmonella enterica*. (Kannan et.al., 2021)

3.5 Anti-fungal activity of Cu, Mn nanoparticles:

The Potato Dextrose Agar Nutrient media was prepared by taking 100ml of distilled water into the conical flask and 1.3gms of nutrient was added to the distilled water in the conical flask mixed properly and 2gms of agar was added to it and mixed. Then a cotton plug was made and the mouth of the conical flask was covered with it. Then the petri dishes were cleaned neatly by using ethanol and they were packed in a cover properly. Then the prepared media and plates were kept in autoclave and they were sterilized at 121°C temperature and 15lbs pressure for 15minutes after reaching the pressure of 15lbs the autoclave was turned off. Then take the petri plate and prepared media out from the Autoclave and they were kept in the cleaned laminar air flow. Then the plates were opened and the media was poured into the plates after mixing the media and the plates were allowed to solidify for 10 to 15 minutes and then the plates were closed.

After the media gets solidified in plates 100µl of the microorganism were taken from the broth and they were spread properly in the plates by using the L shaped rod. Then the wells were made in the plate using the cork borer and they were labeled with the sample numbers and 10µl of the respective Cu and Mn nanoparticles solutions were loaded to the respective wells and the plates were kept in incubator at 37°C for the growth of the microorganism and the anti-fungal activity in the plates was observed and the zone of inhibition was measured around each well and noted down. The anti-fungal activity was done with five fungal organisms like *Aspergillus niger*, *Aspergillus flavus*, *Candida albicans*, *saccharomyces cerevisiae*, *phytophthora infestans*. (Chinnaiah et.,al 2023., Rangayasami et.,al 2020).

Green Synthesis of Cu, Mn NP:-



Fresh leaves of plant



Grinded leaf powder



Figure 1: Sample collection and preparation process

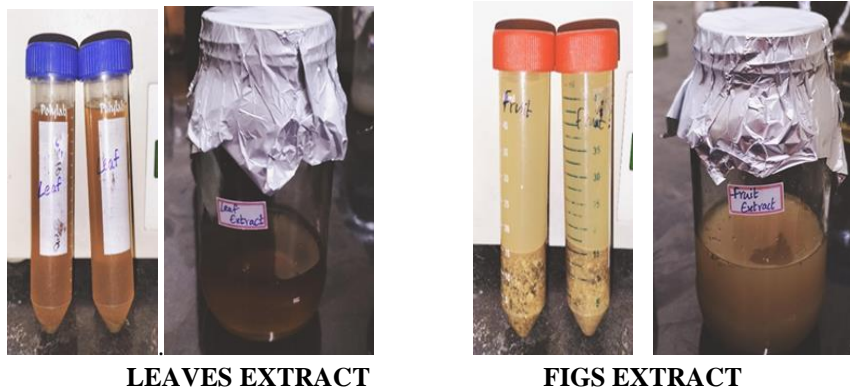


Figure2: Preparation of plant extracts



Figure3: Synthesis of leaf nanoparticles



Figure4: Synthesis of figs nanoparticles

Synthesis of manganese nanoparticles:



Figure 5: Mixtures of leaves and figs after the synthesis of Manganese nanoparticles

4. RESULTS:

4.1 Effect of Different Parameters with UV Visible Spectroscopy on the Production of Copper Nanoparticles:-

Table1: Readings of Leaf Cu NPs at 1:2 concentration ratio with variable pH and temperature

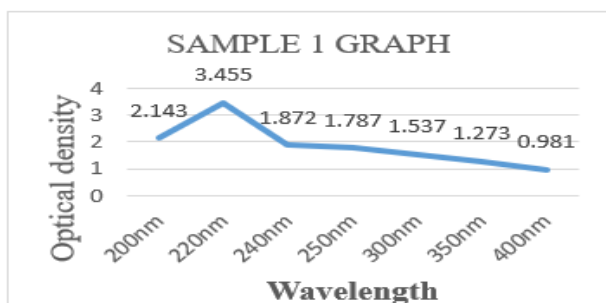
Sample number	Concentration ratio	pH	Temperature (°C)	Optical density at different wavelengths (nm)						
				200	220	240	250	300	350	400
1	1:2	5	50	1.773	3.052	1.443	1.406	0.773	0.400	0.345
2	1:2	5.5	50	3.505	4.000	3.616	3.136	2.618	1.886	1.248
3	1:2	5	70	2.107	3.380	1.825	1.907	1.534	1.209	0.894
4	1:2	5.5	70	2.602	3.960	4.000	3.533	2.658	1.943	1.157

By comparing all the above four samples optical density values of leaf Cu NPs at 1:2 concentration ratio, pH 5.5, Temp 50° of the plant extract and copper sulphate solution high optical density is observed at 220nm range for the samples 1,2,3 and for the sample 4 the high optical density is observed at 240nm range

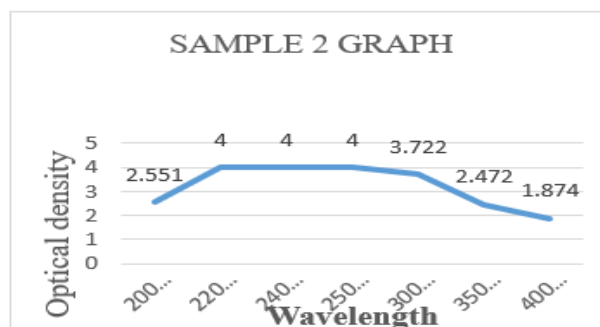
Table3: Readings of Leaf Cu NPs at 1:3 concentration ratio with variable pH and temperature

Sample number	Concentration ratio	pH	Temperature (°C)	Optical density at different wavelengths (nm)						
				200	220	240	250	300	350	400
1	1:3	5	50	2.143	3.455	1.872	1.787	1.537	1.273	0.981
2	1:3	5.5	50	2.551	4.000	4.000	4.000	3.722	2.472	1.874
3	1:3	5	70	1.468	2.797	1.156	1.142	0.978	0.818	0.672
4	1:3	5.5	70	2.660	3.899	2.553	2.801	2.174	1.662	1.109

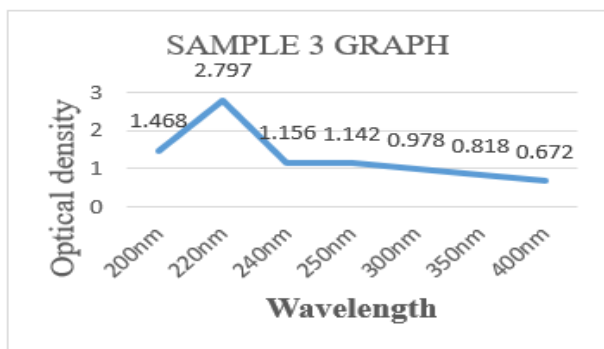
By comparing all the above four samples optical density values of leaf Cu NPs at 1:3 concentration ratio, pH 5.5, Temp 50° of the plant extract and copper sulphate solution high optical density is observed at 220nm range for the samples 1,3,4 and for the sample 2 the high optical density is observed at 220nm, 240nm, and 250nm range.



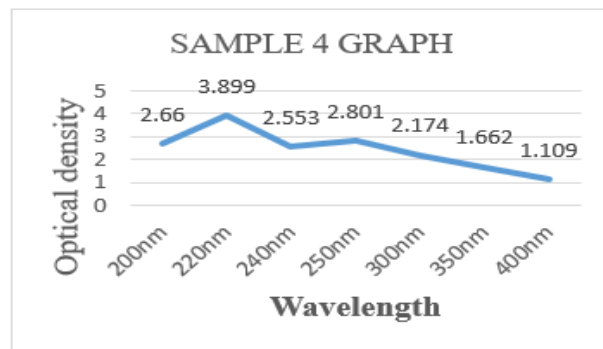
Graph 1: In the sample 1 the high optical density is observed at 220nm range



Graph 2: In the sample 2 the high optical density is observed at 220nm, 240nm and 250nm



Graph 3: In the sample 3 the high optical Density is observed at 220nm range

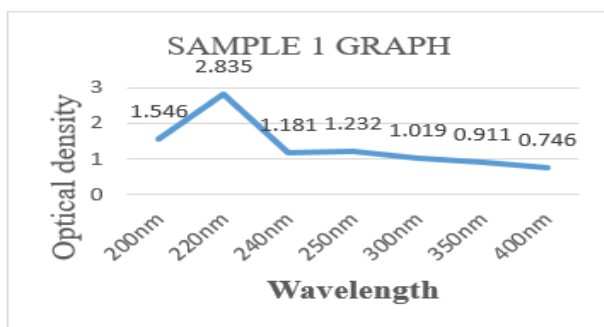


Graph 4: In the sample 2 the high optical density is observed at 220nm range

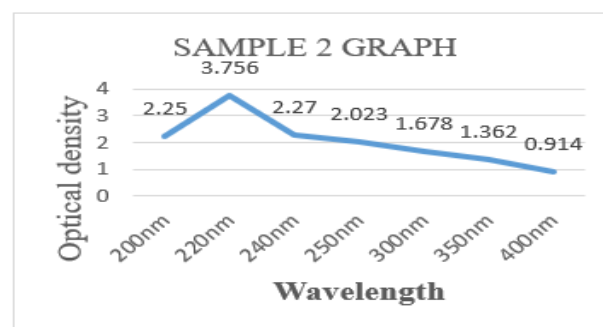
Table4: Readings of Figs Cu NPs at 1:2 concentration ratio with variable pH and temperature

Sample number	Concentration ratio	pH	Temperature (°C)	Optical density at different wavelengths (nm)						
				200	220	240	250	300	350	400
1	1:2	5	50	1.546	2.835	1.181	1.232	1.019	0.911	0.746
2	1:2	5.5	50	2.250	3.756	2.270	2.023	1.678	1.362	0.914
3	1:2	5	70	1.608	2.949	1.319	1.407	1.174	1.073	0.897
4	1:2	5.5	70	1.872	3.137	1.523	1.872	1.742	1.508	1.046

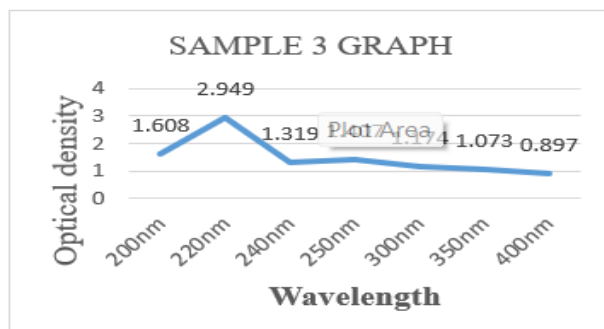
By comparing all the above four samples optical density values of figs Cu NPs at 1:2 concentration ratio of the plant extract and copper sulphate solution high optical density is observed at 220nm range for all the samples 1,2,3,4.



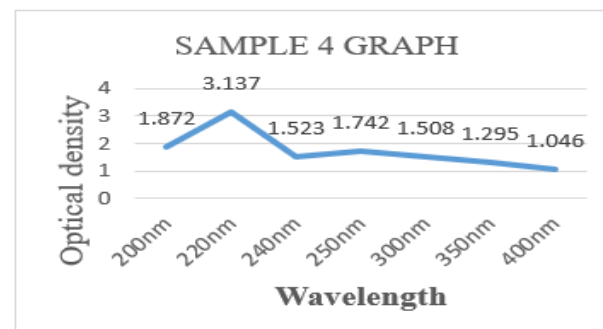
Graph 5: In the sample 1 the high optical Density is observed at 220nm range



Graph 6: In the sample 2 the high optical Density is observed at 220nm range



Graph 7: In the sample 3 the high optical Density is observed at 220nm range



Graph 8: In the sample 4 the high optical Density is observed at 220nm range

Table 5: Readings of Figs Cu NPs at 1:3 concentration ratio with variable pH and temperature

Sample number	Concentration ratio	pH	Temperature (°C)	Optical density at different wavelengths (nm)						
				200	220	240	250	300	350	400
1	1:3	5	50	1.213	2.568	0.914	1.084	0.881	0.792	0.493
2	1:3	5.5	50	1.514	2.836	1.181	0.985	0.88	0.807	0.659
3	1:3	5	70	1.185	2.489	0.799	0.958	0.764	0.682	0.461
4	1:3	5.5	70	1.282	2.619	0.943	0.982	0.580	0.796	0.493

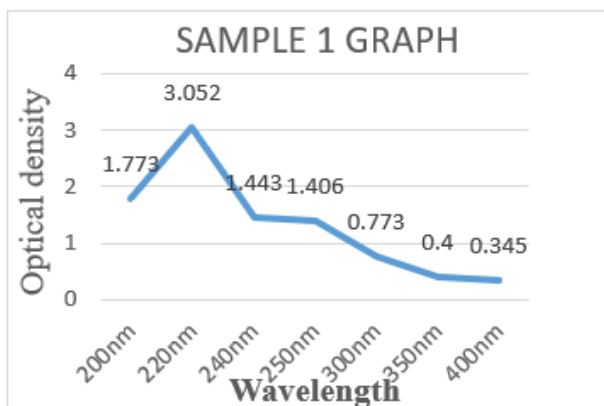
By comparing all the above four samples optical density values of figs Cu NPs at 1:3 concentration ratio of the plant extract and copper sulphate solution high optical density is observed at 220nm range for all the samples 1,2,3,4.

4.2. Effect of Different Parameters with UV Visible Spectroscopy on the Production of Manganese Nanoparticles:-

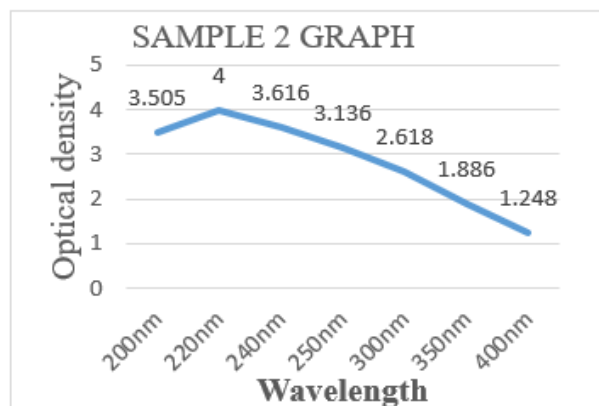
Table2: Readings of Leaf Mn NPs at 0.1gm of MnO₂ with variable pH and temperature

Sample number	Amount of leaf extract (ml) + Conc of MnO ₂ (gm)	pH	Temperature (°C)	Optical density at different wavelengths (nm)						
				200	220	240	250	300	350	400
1	25 + 0.1	7.1	40	0.793	2.122	0.483	0.559	0.445	0.324	0.287
2	25 + 0.1	7.6	40	0.878	2.231	0.595	0.516	0.385	0.345	0.305
3	25 + 0.1	7.1	60	1.003	2.346	0.636	0.377	0.310	0.322	0.273
4	25 + 0.1	7.6	60	0.864	2.211	0.545	0.602	0.491	0.447	0.362

By comparing all the above four samples optical density values of leaf Mn NPs at 0.1gm concentration of MnO₂ high optical density is observed at 220nm range for all the samples 1,2,3,4.



Graph 9: In the sample 1 the high optical Density is observed at 220nm range

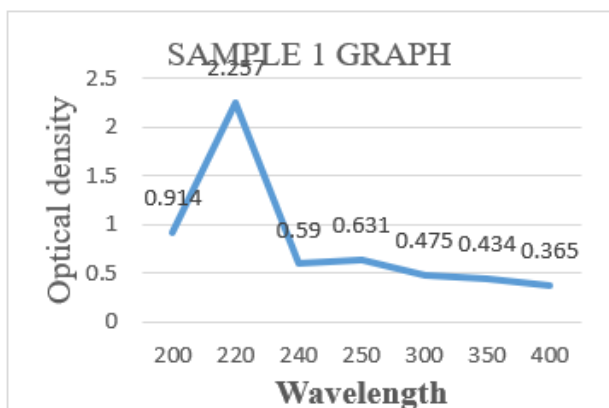


Graph 10: In the sample 2 the high optical Density is observed at 220nm range

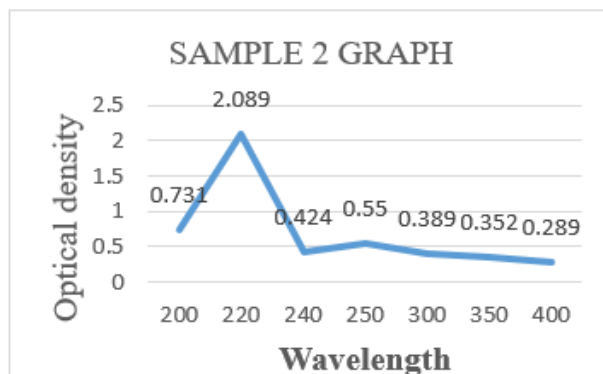
Table 7: Readings of Figs Mn NPs at 0.1gm of MnO₂ with variable pH and temperature

Sample number	Amount of leaf extract (ml) + Conc of MnO ₂ (gm)	pH	Temperature (°C)	Optical density at different wavelengths (nm)						
				200	220	240	250	300	350	400
1	25 + 0.1	7.1	40	0.914	2.257	0.590	0.631	0.475	0.434	0.365
2	25 + 0.1	7.6	40	0.731	2.089	0.424	0.550	0.389	0.352	0.289
3	25 + 0.1	7.1	60	0.867	2.211	0.542	0.705	0.590	0.534	0.464
4	25 + 0.1	7.6	60	0.762	2.101	0.421	0.455	0.387	0.351	0.307

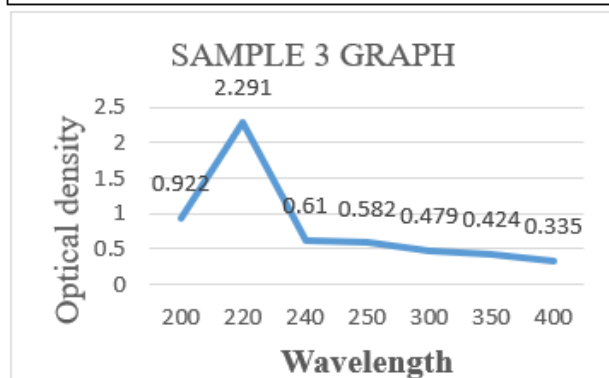
y comparing all the above four samples optical density values of figs Mn NPs at 0.1 gm concentration of MnO₂ high optical density is observed at 220nm range for all the samples 1,2,3,4



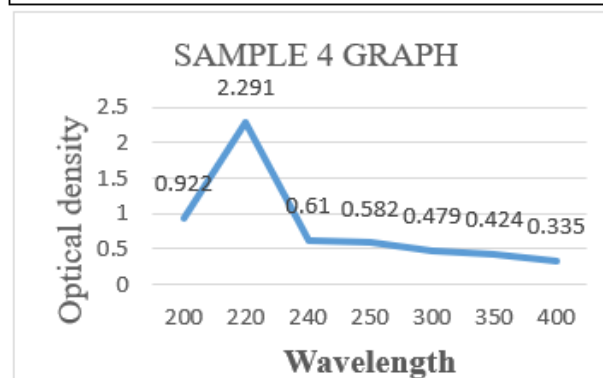
Graph 11: In the sample 1 the high optical Density is observed at 220nm range



Graph 12: In the sample 2 the high optical Density is observed at 220nm range



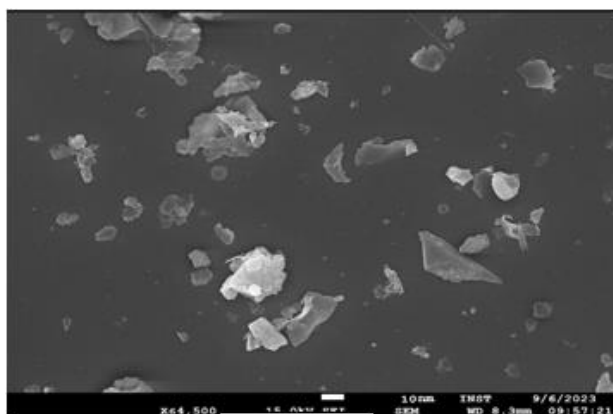
Graph 13: In the sample 3 the high optical Density is observed at 220nm range



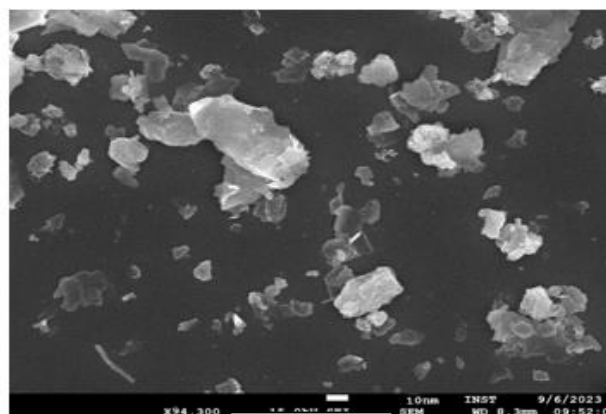
Graph 14: In the sample 4 the high optical Density is observed at 220nm range

SEM Analysis of Cu,Mn NPs:-

Morphology and the size of the Cu NPs were detected using the Scanning Electron Microscope (SEM). It is concluded from given figures that the particles in the samples were compactly arranged and were almost spherical in shape. However, the study shows the size range is 15 nm – 200 nm, with an average size of **80 nm**.

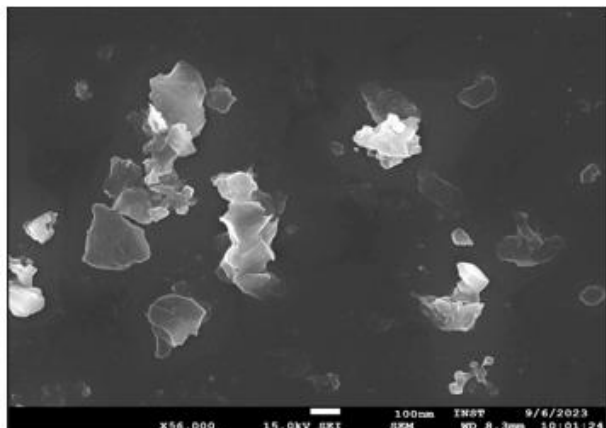


Cu leaf

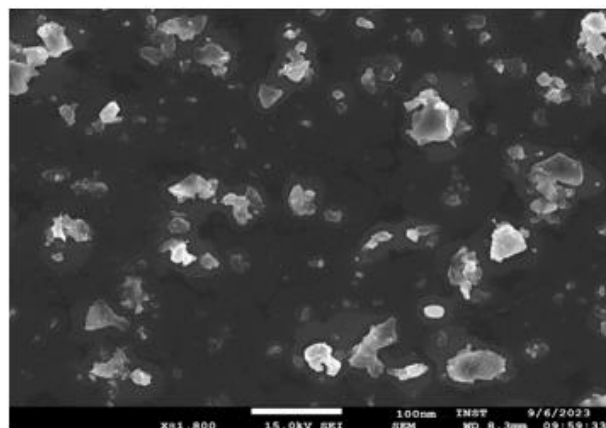


Cu fruit

Morphology and the size of the Mn NPs were detected using the Scanning Electron Microscope (SEM). It is concluded from given figures that the particles in the samples were compactly arranged and were almost spherical in shape. However, the study shows the size range is 60 nm - 280µm, with an average size of **95 nm**.

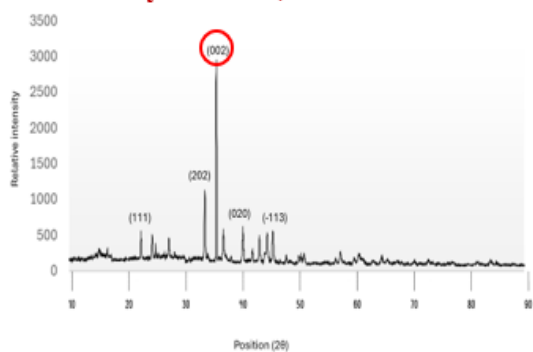


Mn leaf

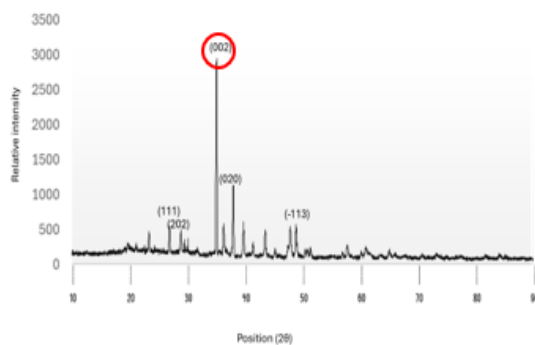


Mn Fruit

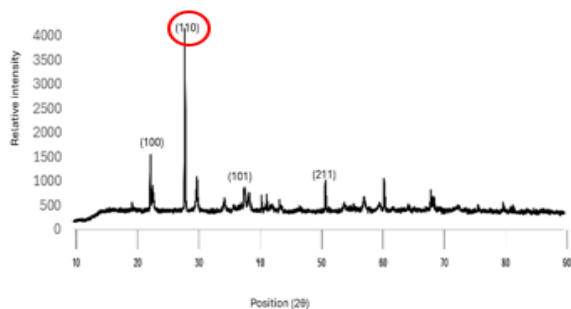
XRD Analysis of Cu, Mn NPs :-



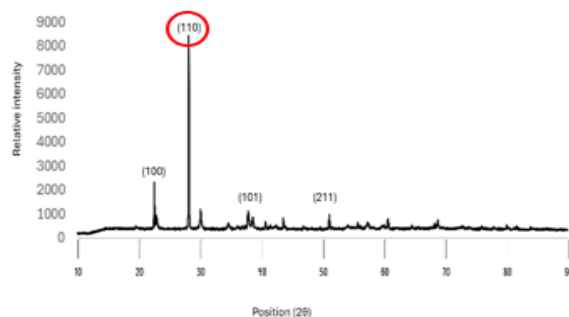
XRD pattern of synthesized Copper Nanoparticles using *T. populinea* leaves extract.
Highest peak is observed $2\theta=35^\circ$



XRD pattern of synthesized Copper Nanoparticles using *T. populinea* fruit extract.
Highest peak is observed $2\theta=35^\circ$



XRD pattern of synthesized Manganese Nanoparticles using *T. populinea* leaves extract.
Highest peak is observed $2\theta=28^\circ$



XRD pattern of synthesized Copper Nanoparticles using *T. populinea* fruit extract.
Highest peak is observed $2\theta=28^\circ$

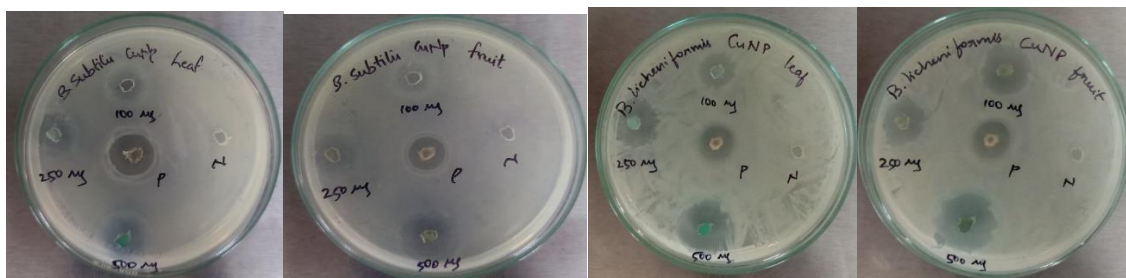
4. Anti-bacterial activity of nanoparticles:

4.1 Activity of Copper nanoparticles:

Effect of Copper NPs on Gram positive bacteria

S.No	organism	Leaf			Fruit		
		100 µg	250 µg	500 µg	100 µg	250 µg	500 µg
1	<i>Bacillus subtilis</i>	15	18	21	14	16	19
2	<i>Bacillus licheniformis</i>	14	16	23	16	18	23
3	<i>Clostridium perfringens</i>	10	15	23	10	20	29
4	<i>Staphylococcus epidermidis</i>	14	16	19	13	15	19
5	<i>Staphylococcus aureus</i>	9	13	15	10	13	16

Cu NPs Isolated from Fruit shows more effect on *Clostridium perfringens* at 500µg inhibitory zone of 29mm



1. Cu NP's activity against *Bacillus subtilis*

2. Cu NPs activity against *Bacillus licheniformis*



3. Cu NPs activity against *Clostridium perfringens*

4. Cu NPs activity against *Staphylococcus epidermidis*

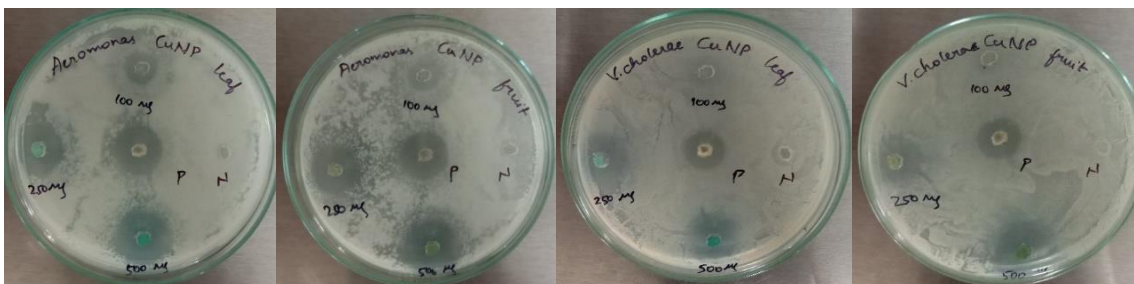


5. Cu NPs activity against *Staphylococcus aureus*

Effect of Copper NPs on Gram negative bacteria

S.No	organism	Leaf			Fruit		
		100 µg	250 µg	500 µg	100 µg	250 µg	500 µg
1	<i>Aeromonas hydrophila</i>	10	14	18	12	18	26
2	<i>vibrio cholera</i>	10	16	19	10	14	18
3	<i>Escherichia coli</i>	14	18	21	13	15	19
4	<i>pseudomonas aeruginosa</i>	15	18	21	12	15	21
5	<i>salmonella enterica</i>	15	17	26	12	15	21

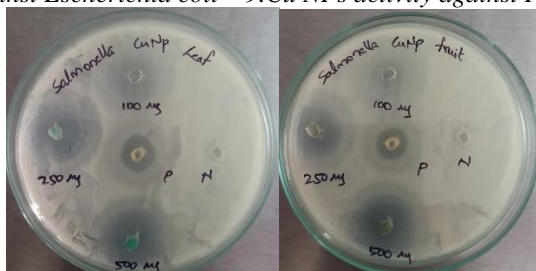
Cu NPs Isolated from Stem shows more effect on *Salmonella enterica* at 500µg inhibitory zone of 29mm



6. Cu NPs activity against *Aeromonas hydrophila* 7. Cu NPs activity against *Vibrio cholerae*



8. Cu NPs activity against *Escherichia coli* 9. Cu NPs activity against *Pseudomonas aeruginosa*

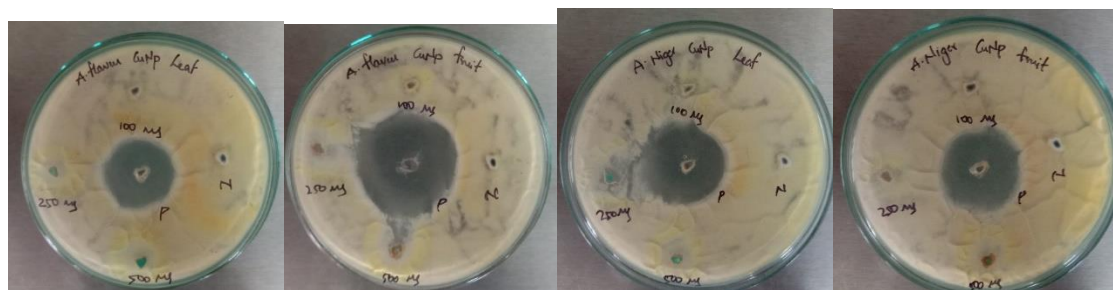


10. Cu NPs activity against *Salmonella enterica*

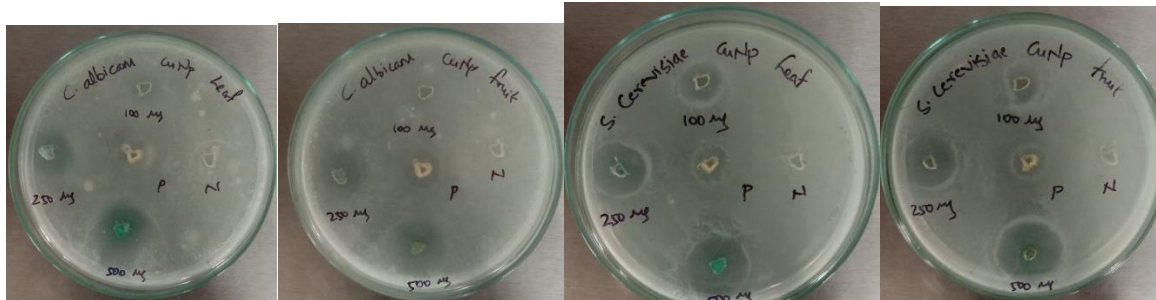
Effect of Copper NPs on fungi

S.No	Organism	Leaf			Fruit		
		100 µg	250 µg	500 µg	100 µg	250 µg	500 µg
1	<i>Aspergillus niger</i>	8	8	9	0	8	9
2	<i>Aspergillus flavus</i>	0	8	8	8	8	9
3	<i>Candida albicans</i>	10	15	18	10	13	17
4	<i>Saccharomyces cerevisiae</i>	8	15	18	8	10	13
5	<i>Phytophthora infestans</i>	13	19	24	15	18	23

Cu NPs Isolated from Leaf shows more effect on *Phytophthora infestans* at 500µg inhibitory zone of 24mm

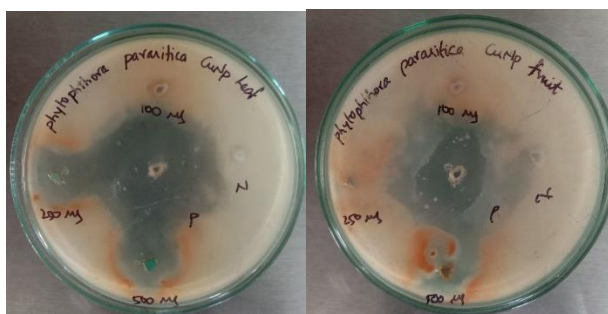


11. Cu NPs activity against *Aspergillus flavus* 12. Cu NPs activity against *Aspergillus niger*



13. Cu NPs activity against *Candida albicans*

15. Cu NPs activity against *Saccharomyces cerevisiae*



14. Cu NPs activity against *Phytophthora infestans*

Effect of Mn NPs on Gram positive bacteria

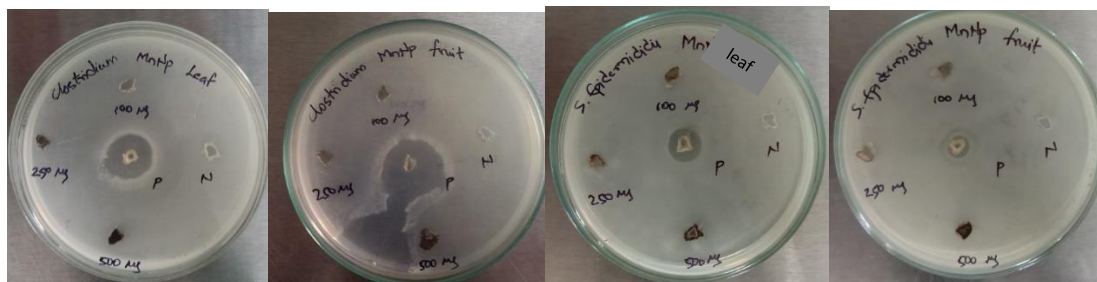
S.No	organism	Leaf			Fruit		
		100 µg	250 µg	500 µg	100 µg	250 µg	500 µg
1	<i>Bacillus subtilis</i>	0	0	0	0	8	10
2	<i>Bacillus licheniformis</i>	0	0	8	0	0	0
3	<i>Clostridium perfringens</i>	0	0	0	0	0	0
4	<i>Staphylococcus epidermidis</i>	0	0	0	0	0	8
5	<i>Staphylococcus aureus</i>	0	0	8	0	0	8

Mn NPs Isolated from Stem shows more effect on *Bacillus licheniformis* at 500µg inhibitory zone of 12mm



1. Mn NP's activity against *Bacillus subtilis*

2. Mn NPs activity against *Bacillus licheniformis*



3. Mn NPs activity against *Clostridium perfringens*

4. Mn NPs activity against *Staphylococcus epidermidis*

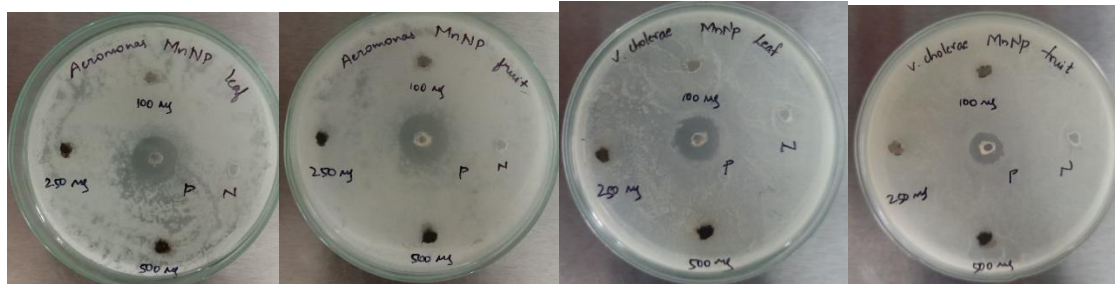


5. Mn NPs activity against *Staphylococcus aureus*

S.No	organism	Leaf			Fruit		
		100 µg	250 µg	500 µg	100 µg	250 µg	500 µg
1	<i>Aeromonas hydrophila</i>	8	8	9	7	8	8
2	<i>Vibrio cholera</i>	0	0	8	0	0	9
3	<i>Escherichia coli</i>	0	7	8	0	8	9
4	<i>Pseudomonas aeruginosa</i>	0	0	0	0	0	8
5	<i>Salmonella enterica</i>	8	8	10	0	0	9

Effect of NPs on Gram negative bacteria

Mn NPs Isolated from Leaf shows more effect on *Aeromonas hydrophila* & *Salmonella enterica* respectively at 500µg inhibitory zone of 10mm



6. Mn NPs activity against *Aeromonas hydrophila* 7. Mn NPs activity against *vibrio cholera*



8. Mn NPs activity against *Escherichia coli*

9. Mn NPs activity against *Pseudomonas aeruginosa*



10. Mn NPs activity against *Salmonella enterica*

Effect of NPs Mn NPs on fungi

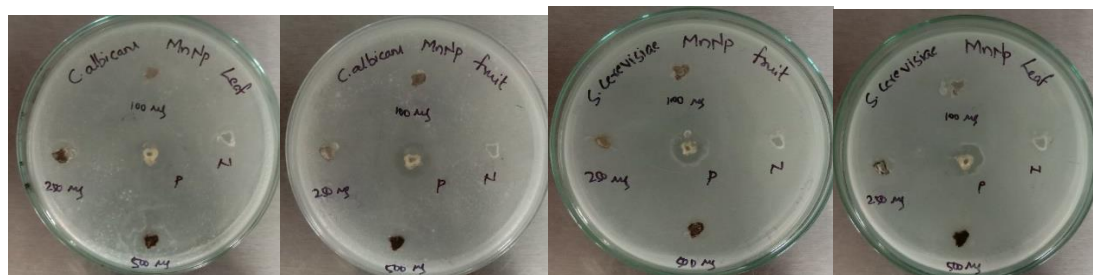
S.No	Organism	Leaf			Fruit		
		100 µg	250 µg	500 µg	100 µg	250 µg	500 µg
1	<i>Aspergillus niger</i>	0	0	0	0	0	0
2	<i>Aspergillus flavus</i>	0	0	0	0	0	0
3	<i>Candida albicans</i>	8	8	10	0	0	8
4	<i>Saccharomyces cerevisiae</i>	0	0	0	0	0	0
5	<i>Phytophthora infestans</i>	0	0	0	0	0	8

Mn NPs Isolated from Leaf shows more effect on *Candida albicans* at 500 µg inhibitory zone of 10mm



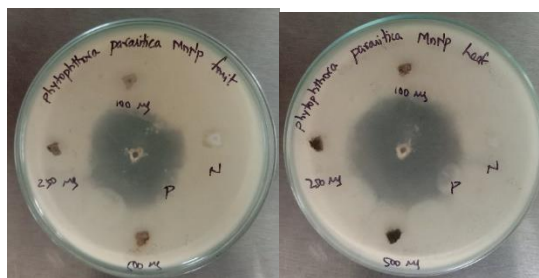
11. Mn NPs activity against *Aspergillus flavus*

12. Mn NPs activity against *Aspergillus niger*



13. Mn NPs activity against *Candida albicans*

14. Mn NPs activity against *Saccharomyces cerevisiae*



15. Mn NPs activity against *Phytophthora infestans*

6. Conclusion:-

The present study shows the synthesis of Cu & Mn NPs at different physical parameters, through disc diffraction methods these NP's acts against upon Gram positive, Gram negative bacteria & Fungi.

7. Acknowledgement

Authors are thankful to the Department of Botany of Andhra University for providing necessary facilities to conduct the studies.

8. References:-

1. L. K. Hakim, M. Yazdanian, M. Alam et al., "Biocompatible and biomaterials application in drug delivery system in oral cavity," *Evidence-based Complementary and Alternative Medicine*, vol. 2021, Article ID 9011226, 12 pages, 2021.
2. J. A. Gerbec, D. Magana, A. Washington, and G. F. Strouse, "Microwave-enhanced reaction rates for nanoparticle synthesis," *Journal of the American Chemical Society*, vol. 127, no. 45, pp. 15791–15800, 2005.
3. J.-P. Jolivet, C. Froidefond, A. Pottier et al., "Size tailoring of oxide nanoparticles by precipitation in aqueous medium. A semi quantitative modelling," *Journal of Materials Chemistry*, vol. 14, no. 21, pp. 3281–3288, 2004.
4. A. K. Gupta and M. Gupta, "Synthesis and surface engineering of iron oxide nanoparticles for biomedical applications," *Biomaterials*, vol. 26, no. 18, pp. 3995–4021, 2005.
5. G. Oberdörster, E. Oberdörster, and J. Oberdörster, "Nanotoxicology: an emerging discipline evolving from studies of Ultrafine particles," *Environmental Health Perspectives*, vol. 113, no. 7, pp. 823–839, 2005.
6. A. Nel, T. Xia, L. Mädler, and N. Li, "Toxic potential of materials at the nanolevel," *Science*, vol. 311, no. 5761, pp. 622–627, 2006.
7. D. Lin and B. Xing, "Root uptake and phytotoxicity of ZnO nanoparticles," *Environmental Science & Technology*, vol. 42, no. 15, pp. 5580–5585, 2008.
8. A. Rastogi, M. Zivcak, O. Sytar et al., "Impact of metal and metal oxide in Chemistry," vol. 5, Article ID 78, 2017.
9. M. Sanchez-Dominguez, M. Boutonnet, and C. Solans, "A novel approach to metal and metal oxide nanoparticle synthesis: The oil-in-water microemulsion reaction method," *Journal of Nanoparticle Research*, vol. 11, pp. 1823–1829, 2009.
10. M. P´erez-Alvarez, G. Cadenas-Pliego, O. P´erez-Camacho, V. E. Compar´an-Padilla, C. J. Cabello-Alvarado, and E. Saucedo-Salazar, "Green synthesis of copper nanoparticles using cotton," *Polymers*, vol. 13, no. 12, p. 1906, 2021.
11. H. Kumar, K. Bhardwaj, R. Sharma et al., "Potential usage of edible mushrooms and their residues to retrieve valuable supplies for industrial applications," *Journal of Fungi*, vol. 7, no. 6, p. 427, 2021.
12. N. A. Lashgari, N. Momeni Roudsari, D. Khayatan et al., "Ginger and its constituents: role in treatment of inflammatory bowel disease," *BioFactors*, vol. 48, no. 1, pp. 7–21, 2022.
13. Velázquez-Salazar, J. J., & Mendoza-Reséndez, R. (2017). Synthesis, Characterization, and Applications of Manganese Oxide Nanoparticles: Recent Advances. *Nanomaterials*, 7(2), 26. <https://doi.org/10.3390/nano7020026>
14. Sharma, D., Kanchi, S., Bisetty, K., & Bisetty, K. (2019). Green Synthesis of Metal Nanoparticles and Their Applications in Environmental Health and Safety. *Environmental Science: Nano*, 6(11), 3323–3367. <https://doi.org/10.1039/c9en00782d>
15. Iravani, S. (2014). Green synthesis of metal nanoparticles using plants. *Green Chemistry*, 16(3), 1238-1260. <https://doi.org/10.1039/C3GC41937H>
16. Saranyaadevi, K., Subbalaxmi, S., Matheswaran, M., Muthukumarasamy, N., & Kumar, S. V. (2014). Synthesis and characterization of copper nanoparticles using Capparis zeylanica L. leaf extract. *Materials Letters*, 132, 303-306.
17. Zhang, H., Li, Y., Wang, T., Zhang, Z., & Wang, Z. (2019). Synthesis and Characterization of Manganese Oxide Nanoparticles with Various Structures and Their Electrochemical Capacitance Performance. *Nanomaterials*, 9(9), 1285. <https://doi.org/10.3390/nano9091285>
18. S. Jin, X. Qi, T. Wang, L. Ren, K. Yang, H. Zhong In vitro study of stimulation effect on endothelialization by a copper bearing cobalt alloy J. Biomed. Mater. Res., 106 (2) (2018), pp. 561-569
19. L. Ren, H.M. Wong, C.H. Yan, K.W.K. Yeung, K. Yang Osteogenic ability of Cu bearing stainless steel J. Biomed. Mater. Res. B Appl. Biomater., 103 (7) (2015), pp. 1433-1444
20. Y. Zhuang, S. Zhang, K. Yang, L. Ren, K. Dai Antibacterial activity of copper-bearing 316L stainless steel for the prevention of implant-related infection J. Biomed. Mater. Res. B Appl. Biomater., 108 (2) (2020), pp. 484-495
21. Y. Chen, H. Cong, Y. Shen, and B. Yu, "Biomedical application of manganese dioxide nanomaterials," *Nanotechnology*, vol. 31, no. 20, Article ID 202001, 2020.

22. Sathishkumar, M., Sneha, K., & Yun, Y. S. (2010). Immobilization of silver nanoparticles synthesized using *Curcuma longa* tuber powder and extract on cotton cloth for bactericidal activity. *Bioresource Technology*, 101(20), 7958-7965. DOI: 10.1016/j.biortech.2010.05.064
23. Narayanan, K. B., & Sakthivel, N. (2010). Green synthesis of biogenic metal nanoparticles by terrestrial and aquatic phototrophic and heterotrophic eukaryotes and biocompatible agents. *Advances in Colloid and Interface Science*, 156(1-2), 1-13. DOI: 10.1016/j.cis.2010.02.001. S. Brunauer, P. H. Emmett, and E. Teller, "Adsorption of gases in multimolecular layers," *Journal of The American Chemical Society*, vol. 60, no. 2, pp. 309–319, 1938.
24. Al-Douri, Y., Abed, A.B., Al-Maamori, M., Aziz, S.B. (2018). Study the optical and electrical properties of PVA:MnO₂ thin films. *Results in Physics*, 10, 920-927.
25. D. B. Williams and C. B. Carter, *Transmission Electron Microscopy: A Textbook for Materials Science*, Springer, 2nd edition, 2009. [ISBN: 978-0-387-76501-3].
26. M. Kuno, "Scanning electron microscopy: Principles and applications," *Oxford Research Encyclopedia of Neuroscience*, Oxford University Press, 2019. [DOI: 10.1093/acrefore/9780190264086.013.133].
27. Kannan, K., Radhika, D., Gnanasangeetha, D., Krishna, L. S. & Gurushankar, K. Y³⁺ and Sm³⁺ co-doped mixed metal oxide nanocomposite: Structural, electrochemical, photocatalytic, and antibacterial properties. *Appl. Surf. Sci. Adv.* **4**, 100085. <https://doi.org/10.1016/j.apsadv.2021.100085> (2021).
28. Chinnaiyah, K., Kannan, K., Krishnamoorthy, R. & Gurushankar, K. *Datura metal* L. leaf extract mediated sodium alginate polymer membrane for supercapacitor and food packaging applications. *Int. J. Biol. Macromol.* **242**, 125112. <https://doi.org/10.1016/j.ijbiomac.2023.125112> (2023).
29. Rangayasami, A., Kannan, K., Joshi, S. & Subban, M. Bioengineered silver nanoparticles using *Elytraria acaulis* (L.F.) Lindau leaf extract and its biological applications. *Biocatal. Agric. Biotech.* **27**, 101690. <https://doi.org/10.1016/j.bcab.2020.101690> (2020).